Population Pharmacokinetics of Romidepsin in Patients with Cutaneous T-Cell Lymphoma and Relapsed Peripheral T-Cell Lymphoma

Sukyung Woo,[1] Erin R. Gardner,[2] Xiaohong Chen,[1] Sandra B. Ockers,[3] Caitlin E. Baum,[3] Tristan M. Sissung,[1] Douglas K. Price,[3] Robin Frye,[4] Richard L. Piekarz,[4] Susan E. Bates,[4] and William D. Figg[1,3]

Abstract

Purpose: Romidepsin is a potent histone deacetylase inhibitor under clinical development. The objective of this study was to evaluate the effect of demographic, clinical, and pharmacogenetic covariates on the pharmacokinetics of romidepsin in patients with T-cell lymphoma.

Experimental Design: Pharmacokinetic assessment was done in 98 patients enrolled in a phase II study who received 14 or 18 mg/m^2 of romidepsin as a 4-hour infusion on day 1 during their first treatment cycle. Population modeling was done using a nonlinear mixed effects modeling approach to explore the effects of polymorphic variations in *CYP3A4, CYP3A5, SLCO1B3*, and *ABCB1*, all of which encode genes thought to be involved in romidepsin disposition.

Results: A two-compartment model with linear kinetics adequately described the romidepsin disposition. Population clearance was 15.9 L/h with between-patient variability of 37%. *ABCB1* 2677G›T/A variant alleles tended toward a reduced clearance and lower volume of tissue distribution, but this was not supported by a statistical significance. Genetic variations in *CYP3A4/5* and *SCLO1B3* had no effect on the systemic exposure.

Conclusion: The population pharmacokinetic analysis indicates moderate interindividual variability in romidepsin pharmacokinetics and no clinically relevant covariates associated with the unexplained pharmacokinetic variability of romidepsin in this population.

Romidepsin (depsipeptide, FK228) is a bicyclic peptide isolated from *Chromobacterium violaceum* (1). Romidepsin has showed potent antitumor activity against many human tumor cell lines (1) and in various xenograft models (2–4), mainly via inhibition of histone deacetylase (HDAC). The acetylation status of histone proteins is important for modulation of gene expression and is highly controlled by the interplay between HDAC and histone acetyltransfereases. Aberrant HDAC activity is believed to be a contributing factor to neoplastic transformation, having been identified in various cancers including leukemia, lymphoma, and solid tumors (5). HDAC inhibitors, a relatively new class of antitumor agents, restore the acetylation of histones and modulate the transcription of genes involved in cell growth, differentiation, and apoptosis. In addition, multiple cellular effects have been described through the increased acetylation of multiple nonhistone proteins. It is not clear which among these effects is most critical for antitumor activity. Romidepsin is currently in phase II clinical trials for the treatment of T-cell lymphoma (6) and advanced solid tumors (7).

There have been multiple phases I trials with romidepsin in patients with refractory solid tumors (8, 9), chronic leukemia and acute myeloid leukemia (10), and T-cell lymphoma (11). A phase II study in 29 patients with refractory metastatic renal cell cancer was conducted, pursuing a major durable response observed in a patient with renal cell cancer in phase I (7); however, no response was observed in this follow-up trials. The maximum-tolerated dose has been established at 17 to 18 mg/m^2 infused over 4 hours on intermittent dosing schedules (8, 9). In general, romidepsin is well-tolerated and dose-limiting toxicities were constitutional symptoms and thrombocytopenia (8–10, 12).

Romidepsin is extensively metabolized *in vivo*, primarily by cytochromes P450 (CYP) 3A4 and to a lesser extent by CYP3A5 (13). A preclinical study in rats showed that 66% of the dose was excreted into the bile (13), a finding thought to be mediated via ATP-binding cassette transporter ABCB1 (P-glycoprotein, MDR1), for which romidepsin has been identified as a substrate (14). Romidepsin is also likely to be

Authors' Affiliations: [1]Clinical Pharmacology Program, Medical Oncology Branch, Center for Cancer Research, National Cancer Institute, Bethesda, Maryland; [2]Clinical Pharmacology Program, Science Applications International Corporation-Frederick, Inc., National Cancer Institute-Frederick, Frederick, Maryland; and [3]Molecular Pharmacology Section, [4]Medical Oncology Branch, Center for Cancer Research, National Cancer Institute, Bethesda, Maryland

Received 8/7/08; revised 12/17/08; accepted 12/30/08.

Grant support: This project has been funded in whole or in part with federal funds from the National Cancer Institute, NIH, under contract N01-CO-12400 (E.R. Gardner). The content of this publication does not necessarily reflect the views or policies of the Department of Health and Human Services, nor does mention of trade names, commercial products, or organizations imply endorsement by the U.S. Government. This research was supported by the Intramural Research Program of the NIH, National Cancer Institute, Center for Cancer Research.

The costs of publication of this article were defrayed in part by the payment of page charges. This article must therefore be hereby marked *advertisement* in accordance with 18 U.S.C. Section 1734 solely to indicate this fact.

Requests for reprints: William D. Figg, Clinical Pharmacology Program, National Cancer Institute, 9000 Rockville Pike, Building 10, Room 5A01, Bethesda, MD 20892. Phone: 301-402-3623; Fax: 301-402-8606; E-mail: wdfigg@helix.nih.gov.

doi:10.1158/1078-0432.CCR-08-1215

Translational Relevance

Romidepsin is one of histone deacetylase inhibitors, an important and promising class of anticancer agents being actively investigated for clinical development. This work reports the first formal assessment of romidepsin pharmacokinetics and potential influence of demographic, laboratory, and genetic variations in relevant drug transporters and metabolic enzymes on romidepsin disposition in cancer patients using a nonlinear mixed effect modeling approach to be able to explain the observed variability in a quantitative manner. A pharmacokinetic model developed will facilitate better understanding of the drug under investigation so that better dosing regimen could be recommended in the future practice of this drug based on patient-specific covariates identified from this study (if any).

a substrate of the organic anion transporter, OATP1B3, an influx transporter encoded by *SLCO1B3* as other cyclic peptides have shown to interact with the same transporter (15, 16). However, the role of single nucleotide polymorphisms (SNP) in *CYP3A4/5*, *ABCB1*, and *SLCO1B3* on individual variability of romidepsin disposition has not been quantitatively assessed.

A phase I trial at the U.S. National Cancer Institute showed significant activity in patients with cutaneous T-cell lymphoma with three partial responses observed and one complete response in a patient with peripheral T-cell lymphoma who received 12.7 or 17.8 mg/m^2 romidepsin i.v. over 4 hours on days 1 and 5 of a 21-day cycle (11). A multi-institutional phase II clinical trial of romidepsin in patients with peripheral T-cell lymphoma or cutaneous T-cell lymphoma is currently ongoing. In this report, we describe the pharmacokinetic assessment of romidepsin in individuals enrolled on the current phase II trial at the National Cancer Institute. The main objectives of this analysis were to estimate romidepsin pharmacokinetic variables and their variability in patients with T-cell lymphoma and to evaluate the effect of polymorphic variants in genes involved in romidepsin disposition as well as patient-specific variables to individual systemic exposure on romidepsin using a population modeling approach.

Materials and Methods

Patients and study design. This was a multi-institutional phase II clinical trial evaluating the safety and efficacy of romidepsin. Patients included in this analysis were treated at one of nine clinical sites, primarily the National Cancer Institute and the Peter MacCallum Cancer Centre. The clinical protocols were approved by the institutional review board of each institute, and all patients provided informed consent before study participation. Enrollment was limited to patients ages 18 y or older with relapsed or refractory cutaneous or peripheral T-cell lymphoma. Patient eligibility and exclusion criteria have been previously reported (6). The first 5 patients were treated on days 1 and 5 of a 21-d cycle at a starting dose of 18 mg/m^2 given as an i.v. infusion over 4 h. Subsequently, for improved patient tolerability, romidepsin was administered on days 1, 8, and 15 of a 28-d cycle at a starting dose of 14 mg/m^2 (12).

Pharmacokinetic sampling and analytic method. Pharmacokinetic assessment of romidepsin was done only on day 1 of cycle 1. Blood samples for pharmacokinetic evaluation were obtained before drug administration and at the end of infusion (4 h) as well as at 2, 7, 9, 11, 14, and 18 h after completion of infusion. Samples were collected into tubes containing heparin as an anticoagulant and immediately placed on ice. After centrifugation for 5 min at 1200 $\times$ *g*, the plasma was transferred to a cryovial and stored at -80°C until analysis.

Plasma concentrations of romidepsin were determined by liquid chromatography with single-quadruple mass spectrometric detection with a lower limit of quantitation of 2 ng/mL and the lower limit of detection of 1 ng/mL (17). The accuracy and precision of the assay were <6.4% and 3.5%, respectively. The assay was done in the Clinical Pharmacology Program of the National Cancer Institute.

Genotyping analysis. Genomic DNA was extracted from plasma using a QiaBlood DNA extraction kit (Qiagen) and stored at 4°C. Genotyping was done via direct sequencing at three *ABCB1* loci (1236 C>T, 2677 G>T/A, and 3435 C>T; 18), *CYP3A4*1B* (19), *CYP3A5*3* (19), and *SLCO1B3* 334T>G (OATP1B3 S112A; ref. 20) as previously described. Direct nucleotide sequencing PCR was conducted using the Big Dye Terminator Cycle Sequencing Ready Reaction kit V1.1 on an ABI Prism 3130 xl Genetic Analyzer (Applied BioSystems). The most likely *ABCB1* diplotype was computed in the Caucasian and African-American population separately using an EM algorithm (Helix Tree), and diplotypes were grouped for comparison with romidepsin pharmacokinetics using a previously reported method (18).

Population pharmacokinetic analysis. Population pharmacokinetic model development and simulation were done using the nonlinear mixed effects modeling (NONMEM) VI level 2.0 (Globomax; ref. 21). NONMEM was complied by Intel Visual Fortran compiler (version 10; Intel Corporation) on the Windows XP operating system. Data processing and statistical and graphical analyses including evaluation of NONMEM outputs were done using S-PLUS (7.0, Insightful).

Initially, the base pharmacokinetic model that best described the romidepsin concentration-time profiles without consideration of patient-specific covariates was developed. A transform-both-side approach was used by taking the logarithm of observed and model predicted concentrations of romidepsin. Individual dose was entered as milligram of romidepsin in the NONMEM database. Two different basic structure models, two- and three-compartment pharmacokinetic model with i.v. infusion and first-order elimination, were compared characterize romidepsin disposition. As one third of patients showed a half of their concentrations fell below the limit of detection, use of YLO option available in NONMEM VI was also explored to avoid a potential bias in model misspecification resulting from the censoring data below limit of detection (22). YLO was set to be equal to the log-transformed

Table 1. Patient characteristics

Variable	Values
Age (y)	55.1 ± 12.4 (27-79)
Body weight (kg)	82.8 ± 18.6 (44.9-126)
BSA (m^2)	1.94 ± 0.23 (1.41-2.46)
Albumin (g/dl)*	3.5 ± 0.6 (1.9-4.6)
Creatinine (mg/dl)*	0.9 ± 0.2 (0.4-2.4)
Sex	
Male	63
Female	35
Race	
White	75
African-American	17
Hispanic	3
Asian	3
T-cell lymphoma type	
Cutaneous	64
Peripheral	34

*Values for 7 out of 91 patients were not known.

Table 2. Patient genotypes

Polymorphism	Genotype frequencies		
	Wt	Het	Var
CYP3A4*1B	79	8	11
CYP3A5*3C	11	16	71
ABCB1 1236C>T	33	43	22
2677G>A/T*	32	42/3 (GT/GA)	16/4 (TT/AA)
3435C>T	30	42	26
SLCO1B3 S112A †	15	24	57

Abbreviations: Wt, homozygous wild-type patient; Het, heterozygous variant patient; Var, homozygous variant patient.
*(n = 1).
†(n = 2) unable to genotype.

limit of detection. The first-order conditional estimation method with LAPLACIAN option was used. Interindividual variability for the pharmacokinetic variables was modeled using the following exponential error term:

$$P_i = P_{pop} \cdot \exp(\eta_{Pi})$$

where P_i is the ith individual's variable, P_{pop} is the mean population variable, and η_{pi} represents the shift of the variable of the ith individual from the population mean. η_p is random variable with mean zero and variance of $\omega^2{}_p$, which is estimated as part of the population model. Correlation between each term was also evaluated using a BLOCK covariance matrix. An additive error model was use to describe residual variability:

$$Y_{ij} = F(P_i, t_{ij}) + \varepsilon_{ij}$$

where Y_{ij} denotes the jth observation for the ith subject, $F(P_i, t_{ij})$ is the predicted value of the data from the model with a vector of the individual pharmacokinetics variables for the ith subject (P_i) at a time t_{ij}. The ε_{ij} is the residual difference between the predicted and the observed value. A combined additive and proportional error model was also evaluated.

After establishing an appropriate structure model, the covariate screening was guided by graphical assessments and stepwise linear regression of relationships between the individual variable estimates (η_{pi}) and each of the covariates. A statistical significance of potential covariates identified from the screening analysis was tested one by one by including in the population model. Covariates evaluated for their possible influence on pharmacokinetic variables included age, weight, body surface area (BSA), sex, albumin, serum creatinine concentration, and types of T-cell lymphoma. In addition, effects of genotypes of *ABCB1*, *CYP3A4/5*, and *SLCO1B3* in individual patients were explored in relation to romidepsin disposition. Missing values for the continuous covariates were imputed using the median value in each variable. The frequency of missing covariates was <10%. Genotype information was coded as an index variable. For individuals with missing genotype information, a dummy variable MISS was used to set equal to 1, and otherwise 0. For a binary covariate, for example, the covariate model was defined as TVCL = $\theta_1 + \theta_2 \cdot (1\text{-MISS}) \cdot \text{GENT} + \theta_3 \cdot \text{MISS}$, where GENT indicates genotype status being equal to 0 for wild-type patients and 1 for heterozygous or homozygous variant type patients. Thus, θ_1 is the typical value for individuals carrying the wild-type alleles, $\theta_1 + \theta_2$ for carriers of one or two variant alleles, and $\theta_1 + \theta_3$ for those with missing genotype. If the value of θ_3 was not significantly different from zero, it was set to zero.

In model development, model selections were guided by the typical goodness-of-fit diagnostic plots, precisions of variable estimates, and model objective function value (OFV) used in the likelihood ratio test. Alternative hierarchical models were discriminated based on a reduction of OFV of at least 6.63 points, which corresponds to a significance level of P value of <0.01 for models that differ by one variable.

Model evaluation. The predictive check and nonparametric bootstrap were used as methods of model evaluation. The bootstrap analysis was done to assess 95% confidence interval of the model variable estimates using the bootstrap option in the software package Wings for NONMEM (N. Holford; Version 613). One thousand five hundred bootstrap data sets were obtained and fitted with the same model to obtain variable estimates for each replicate. The 2.5th and 97.5th values of each variable were used to compute the lower and upper boundary of bootstrap 95% confidence interval and compared with the model estimates from NONMEM.

The predictive check was used to evaluate the predictive performance of the model (23). The model-derived simulations for 10,000 virtual patients were done using the variable estimates from the final model. The median (50% quartile) and 5% and 95% percentiles from the simulated data were chosen to compare with the observed romidepsin concentrations.

Results

Patient demographics and genotypes. A total of 98 patients with either cutaneous T-cell lymphoma (n = 64) or peripheral T-cell lymphoma (n = 34) completed a pharmacokinetic study

Table 3. *ABCB1* diplogtype groupings

Diplotype	Chromosome 1			Chromosome 2			Frequency (%)
	1236C>T	2677G>T/A	3435C>T	1236C>T	2677G>T/A	3435C>T	
Diplotype 1	C	G	C	C	G	C	15 (16.9)
Diplotype 2	C	G	C	*	*	*	26 (29.2)
Diplotype 3	C	G	C	T	T	T	21 (23.6)
Diplotype 4	T	T	T	*	*	*	16 (18)
Diplotype 5	T	T	T	T	T	T	11 (12.4)
Diplotype 6	—	G	C	—	G	C	19 (21.3)
Diplotype 7	—	G	C	—	†	†	18 (20.2)
Diplotype 8	—	G	C	—	T	T	27 (30.3)
Diplotype 9	—	T	T	—	†	†	12 (13.5)
Diplotype 10	—	T	T	—	T	T	13 (14.6)

NOTE: Diplotype were grouped based on the previous approaches to reflect whether or not individual carried a fully wild-type or fully variant halplotype (21, 25). * and †, any combination of alleles that is not mutually exclusive with another diplotype consisting of all 1236-2677-3435 SNPs and 2677-3435 SNPs, respectively. 1236 SNP was not considered in calculation of the diplotypes 6 to 10.

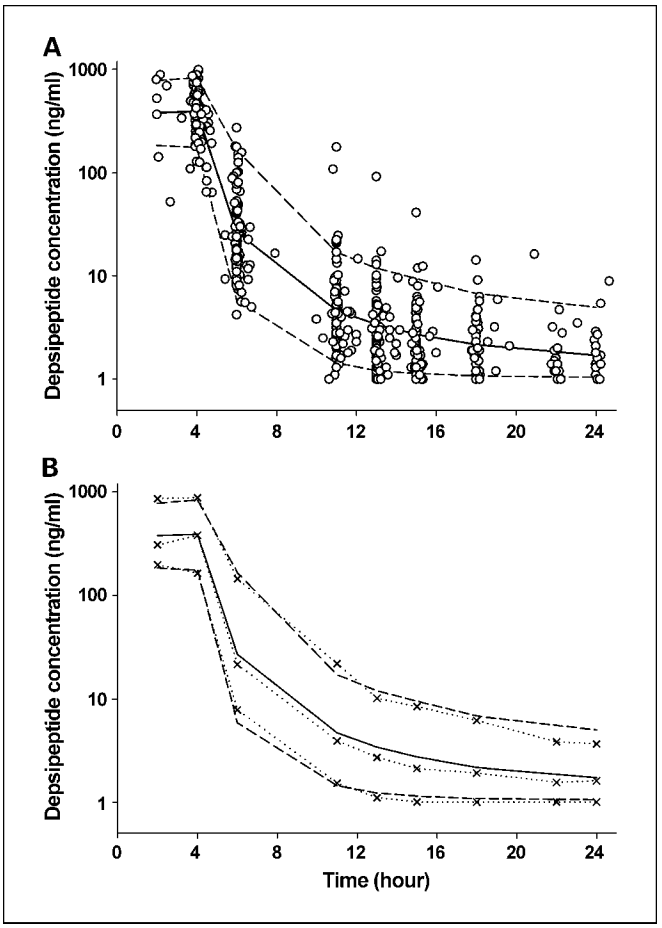

Fig. 1. Visual predictive check for the final pharmacokinetic model. *Open symbols,* observed plasma concentrations of romidepsin from all patients following 4-h infusion of romidepsin 14 mg/m^2 on day 1. Median (*solid line*) and 90% prediction intervals (*broken lines*) from model-derived simulations. *Dotted lines with symbols,* the 5th, 50th, and 95th percentiles of observations.

of romidepsin on day 1 during cycle 1 of therapy. The demographic characteristics of patients in this study are listed in Table 1. Patients consisted of 63 males and 35 females with a mean age of 55.1 years (27-79 years) and a mean body weight of 82.8 kg (44.9-126 kg). Genotypes and allele frequencies for *CYP3A4*, *CYP3A5*, *ABCB1*, and *SLCO1B3* are reported in Table 2. One patient for *ABCB1* 2677G>T/A and two patients for *SLCO1B3* 334T>G were not genotyped due to difficulty in PCR amplification. All genotype frequencies were in the Hardy-Weinberg equilibrium, except for *ABCB1* 3435C>T in African-American population (P = 0.013). Table 3 lists 10 diplotypes inferred from the *ABCB1* SNPs. Diplotypes 1 to 5 were constituted from the *ABCB1* 1236C-2677G-3435C, ranking them in order of increasing genetic variation. Similarly, diplotypes 6 to 10 were computed based on *ABCB1* 2677G-3435C. Diplotype data were available for 89 of 98 patients due to individuals with missing genotype information (n = 3) and small numbers of subjects in Hispanic (n = 3) and Asian (n = 3) populations. Associations between these diplotypes and romidepsin disposition were explored in subsequent analyses.

Population pharmacokinetic model. Figure 1 shows romidepsin plasma concentration versus time profiles observed in all patients who received a 4-hour infusion of romidepsin at a dose of 14 mg/m^2 on day 1. After the end of the infusion, romidepsin rapidly decreased and exhibited a polyexponential decline. The number of observations ranged 2 to 9 per subject with a median of 6. A total of 531 concentrations from 98 patients provided the pharmacokinetic data for model development.

When two- and three-compartment models were compared, an improvement from a three-compartment model was minimal compared with a two-compartment model with YLO variable (ΔOFV = 8.7). Without the YLO, the three-compartment model was favored over two-compartment model, resulting in the reduction in OFV by 108 points. However, it was evident that the concentration data were censored by the analytic detection limit and the YLO option was needed to overcome a possible bias from such data. No particular dose-dependency in pharmacokinetic variables toward 18 mg/m^2 was observed. Therefore, the two-compartment model with linear elimination was chosen as the structural pharmacokinetic model for romidepsin. A between-subject variability term expressed as an exponential model was incorporated into systemic clearance (CL), central volume of distribution (V1)

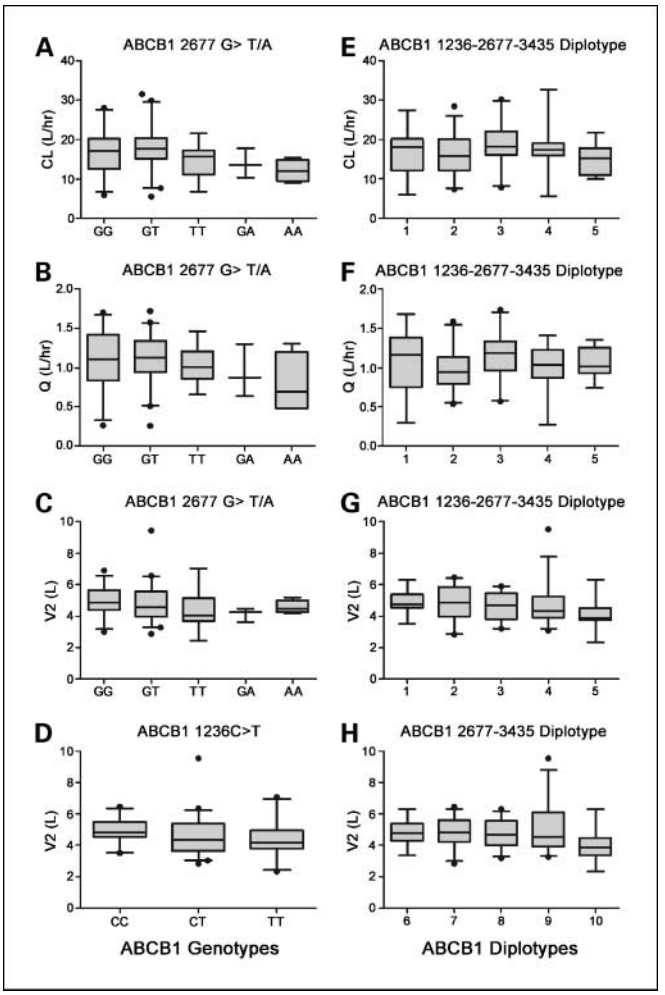

Fig. 2. Box-whisker plots of the association between *ABCB1* polymorphisms and romidepsin pharmacokinetic parameters. *Whiskers below,* 5th percentile; *whiskers above,* 95th percentiles; *lines in the middle,* median values. Diplotypes 1 to 10 are defined in Table 3.

and intercompartmental clearance (Q), and peripheral volume of distribution (V2). Although there were no apparent trends observed between individual variables (η_{pi}) and size-related variables (e.g., height, weight, or BSA), BSA was used as a size measurement and included on CL as a proportional term relative to the median value ($\overline{BSA}$ = 1.935 m^2). The addition of BSA increased the OFV slightly by 2.15 points but remained for clinical relevance. Any association of other demographic variables and laboratory values with romidepsin pharmacokinetics was not noticed.

Of the three *ABCB1* loci tested in this study, individuals carrying *ABCB1* 2677TT, 2677GA, or 2677AA trended toward a lower clearance compared with individuals carrying only reference alleles or *ABCB1* 2677GT genotypes (P = 0.077; degrees of freedom = 4; one-way ANOVA) as shown in Fig. 2A. The similar trend was also observed for intercompartmental clearance (Q), although it might be attributed to high correlation observed between CL and Q (r = 0.781; Table 4). It seemed that sequence variations in *ABCB1* also affected the volume of distribution. The volume of tissue distribution for romidepsin (V2) tended to be lower in individuals with *ABCB1* 2677 TT genotype or 1267 variant alleles (CT and TT) than those with alternative genotypes (Fig. 2C-D). However, significance of these *ABCB1* genotypes on CL, Q, or V2 was not confirmed by statistical criteria. For carriers of 2677 GA/AA compared with noncarriers, a noticeable difference in CL between 2 groups seemed to be present (13 versus 16 L/h) but did not reach the statistical criteria (ΔOFV = 3.4), presumably due to a small number of patients for this particular group (n = 7). Given that others have found associations of *ABCB1* haplotypes with drug transport (24) and drug disposition (18, 25–27), we tested for similar associations between romidepsin disposition and *ABCB1* diplotype. As shown in Fig. 2G to H, a noticeable difference toward lower V2 was seen in patients carrying only variant alleles at both 2677 and 3435 SNPs (diplotype 10) or at all 3 *ABCB1* SNPs (diplotype 5) than in carriers of alternative diplotypes with unadjusted P value of 0.023 to 0.026, but it did not lead to a significant reduction in OFV when tested by coding as GENT of 0 for diplotypes 1 to 4 (or diplotypes 6-9) and GENT of 1 for diplotype 5 (or diplotype 10). No association was found between any *ABCB1* alleles or diplotypes and the central volume of distribution. Values of romidepsin clearance were comparable between patients carrying reference alleles and individuals carrying one or more *CYP3A4*1B* or *CYP3A5*3C* allele (data not shown). Genotypes of *SLCO1B3* were not correlated with any pharmacokinetic variables. Thus, the two-compartment model including BSA on CL constituted the final pharmacokinetic model for romidepsin in this population. The final model was further refined by evaluating correlations between random interindividual effects based on graphical and statistical methods and implementing in a variance-covariance matrix. The correlation between CL and Q (r = 0.781) and between Q and V1 (r = -0.588) were found to be relevant.

The diagnostic plots for the final model showed that predicted and observed data well agreed (Fig. 3). The individual weighted residuals did not reflect any systematic trends. The pharmacokinetic variable estimates resulting from the final model are provided in Table 4. For a patient with BSA of 1.935 m^2, the typical population clearance (CL) was estimated at 15.9 L/h and the central volume of distribution at 10 L. In adult, the mean value of CL was reported as 10.5 L/h/m^2 at 17.8 mg/m^2 (9), similar to our estimation (8.8 L/h/m^2) expressed in terms of BSA-normalization. The estimated elimination half-life was 3.5 hours, which is comparable with the previously reported value (8, 10). Interindividual variability in pharmacokinetic variables was moderate in this population, with percent coefficient of variation (%CV) ranging 30% to 40%. The random residual constant coefficient of variation was ~29%.

The evaluation of the final pharmacokinetic model was done using a predictive check and a nonparametric bootstrap. The results of predictive performances of the final model are shown in Fig. 1. It depicts the median and 90% prediction interval of the model-based prediction for plasma concentration-time profiles in comparison with the observed romidepsin plasma concentrations, suggesting that the final model accurately reflects the data. The nonparametric bootstrap analysis provided 95% confidence interval for the parameter estimates. The confidence intervals presented in Table 4 were based on

Table 4. Pharmacokinetic parameters of romidepsin estimated from the final model

Parameter	NONMEM estimate	Bootstrap analysis	
		Median (%RSE)	95% CI
CL (L/h)	15.9*	15.9 (6.2)	14.0 - 17.7
V1 (L)	10	9.71 (8.9)	7.8 - 11.2
Q (L/h)	0.996	1.01 (14.7)	0.80 - 1.40
V2 (L)	4.72	4.73 (11.1)	3.92 - 5.93
BSV_{CL} (%CV)	37.1	36.6 (11.8)	28.5 - 45.1
BSV_{V1} (%CV)	39.0	38.9 (25.9)	23.2 - 63.1
BSV_{Q} (%CV)	39.6	39.5 (22.8)	24.9 - 60.1
BSV_{V2} (%CV)	28.9	28.2 (22.6)	16.3 - 40.8
$Corr_{CL-Q}$	0.781	0.781 (18.6)	0.394 - 0.928
$Corr_{Q-V1}$	-0.588	-0.541 (28.7)	-0.748 - -0.203
Residual error (%CV)	28.6	29.3 (10.5)	24.4 - 36.3

Abbreviations: %RSE, relative standard error of parameter estimate; CI, confidence intervals; BSV, between subject variability in parameters; %CV, percent of coefficient of variation; Corr, correlation between individual parameters.
*CL = 15.9 × (BSA/1.935). Typical value of CL for a patient with BSA = 1.935 m^2.

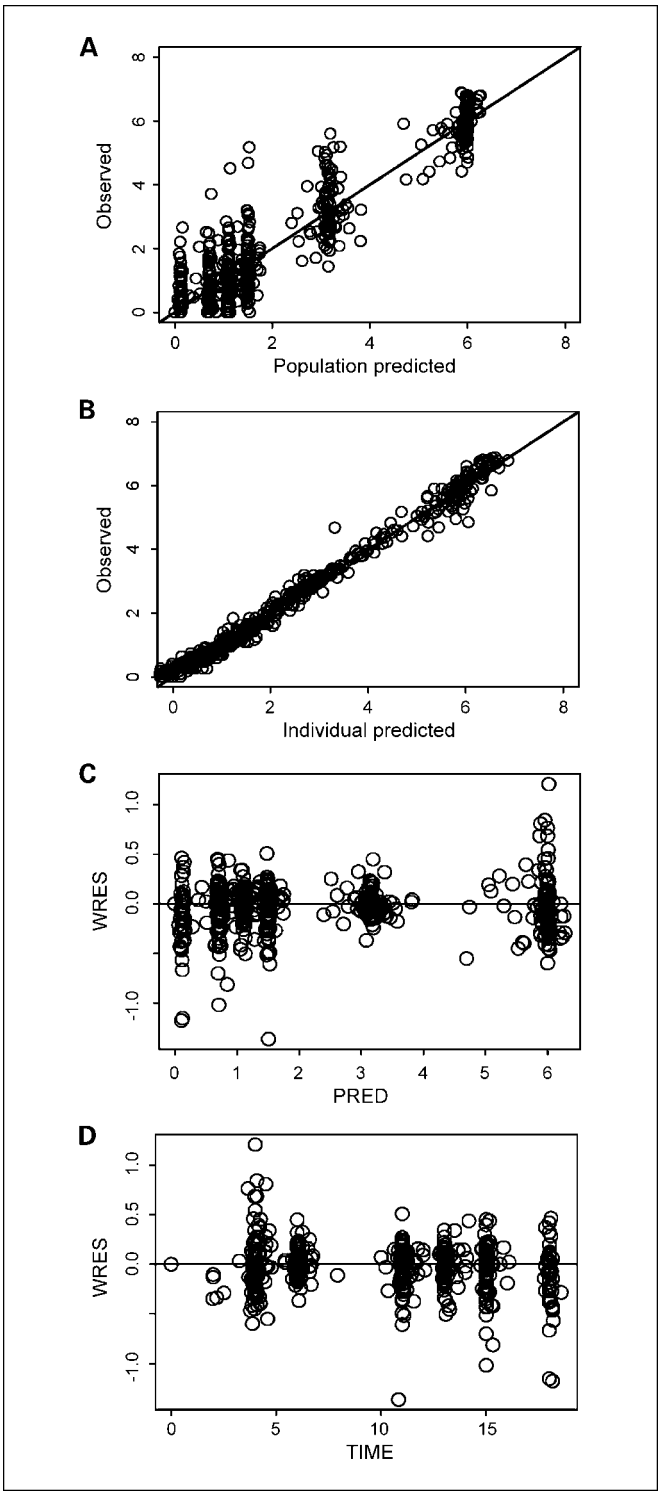

Fig. 3. Goodness-of-fit plots for the final model: scatter plots of the observed versus the population predictions (*A*) and the observed versus the individual model predictions of romidepsin concentrations (*B*); scatter plots of the individual weighted residuals with respect to the population model predictions (*C*) and time (*D*).

1,342 bootstrap estimates that converged successfully from 1,500 runs, regardless of $COVARIANCE step success. The majority of runs terminated during minimization were due to rounding errors and parameter estimates from these terminated runs were not significantly different from others with successful convergence. In general, the observed bootstrap medians were consistent with the typical population model parameters as well as random effect parameters and the 95% confidence interval for these parameters were relatively small, indicating reliability of the parameter estimates from the final model. Although the first-order conditional estimation with LAPLACIAN method failed to estimate SE for the parameter estimates, the precision of these NONMEM estimates seemed to be reasonable because the relative SE from the bootstrap analysis was lower than 30%.

Discussion

Romidepsin is a potent HDAC inhibitor currently under clinical development for advanced hematologic and solid tumors. Responses in patients enrolled on a phase I study showed that romidepsin is a potentially effective therapy in T-cell lymphoma (9). This study describes characteristics of romidepsin pharmacokinetics in patients enrolled in a phase II multi-institutional trial with romidepsin for cutaneous T-cell lymphoma and peripheral T-cell lymphoma, whose doses were 14 or 18 mg/m^2 on day 1 during their first treatment cycle.

After a 4-hour infusion, romidepsin was rapidly cleared from the circulation with a short half-life of ~3.5 hours, as observed in other studies with romidepsin (8, 10). The disposition of romidepsin has been shown to follow a polyexponential decline and has previously been described by a two-compartment pharmacokinetic model (8–10). Although dose proportionality has not been formally assessed before, no apparent nonlinearity has been reported for romidepsin disposition within the range of 1 to 24.9 mg/m^2 (8, 9). The pharmacokinetics of romidepsin does not seem to be affected by repeated dosing (9). The reported value of total clearance for romidepsin in adults is 4.8 L/h/m^2 at the dose of 13 mg/m^2 (10) and 10.5 L/h/m^2 at 17.8 mg/m^2 (9). A phase I study conducted in pediatric patients (median age of 13 years; ranged 2-21 years) with refractory solid tumors who received romidepsin as a 4-hours infusion at 17 mg/m^2 determined a median CL of 6.8 L/h/m^2 (8). The value of the BSA-normalized clearance (8.8 L/h/m^2) in adults (median age of 55 years; ranged 27-79 years) from our study was slightly higher than one in pediatric patients, but the reported values including ours were comparable each other and within the range. Thus, inclusion of BSA in CL as a size measurement seems reasonable for clinical relevance. As our analysis did not find any association of age with CL, it seems that age is not a significant predictor for CL of romidepsin.

In the present study, we evaluated the relative contribution of polymorphisms in metabolizing enzymes and transporters of romidepsin to the pharmacokinetics. Although romidepsin undergoes extensive metabolism by CYP3A4 and CYP3A5, their gene sequence variations did not affect romidepsin pharmacokinetics. A recent study showed that Caucasian patients carrying a copy of both *CYP3A4*1B* and *CYP3A5*1A* (e.g., those who presumably carry a functional *CYP3A5* gene) had an increased docetaxel clearance (28). Of 75 Caucasians in our study, there were only 3 individuals categorized into this group and their clearance did not differ from remaining patients.

Studies have shown that variant alleles in *ABCB1* alter protein folding, function, and/or expression level in different

types of tissues (24, 26, 27). For example, the variant alleles at loci 2677 and 3435 of *ABCB1* have been associated with lower expression of hepatic ABCB1 (29). Thus, it was hypothesized that polymorphisms in *ABCB1* may result in reduced transport of romidepsin into bile, thereby resulting in decreased overall clearance. A tendency toward lower CL was seen in patients carrying *ABCB1* 2677 variant alleles, especially for individuals carrying one or more 2677A alleles, compared with those carrying the reference alleles. However, the allele frequency for 2677A is relatively low (7 of 98 patients in the current study possessed at least one A allele), which compromises the power for statistical comparisons. *ABCB1* variants at 1236C>T and 3435C>T lacked any significant association with romidepsin clearance. Sequence variations in *ABCB1* gene are also expected to alter distribution of its substrates, thereby affecting the tissue concentrations in a more complicated manner. The genetic alterations at 2677G>T/A and/or 3435C>T have shown to be associated with lowered ABCB1 expression in liver (29) and intestines (30), whereas 2677AT and TT genotypes have been correlated with higher expression of ABCB1 in heart (31). Given the tissue-dependent modulation of ABCB1 expression by polymorphic variations, it may be difficult to identify an association between genotypes and the overall distributional parameters (V2 or Q) unless drug levels in pertinent tissues were directly measured. Nevertheless, we observed the reduced volume of tissue distribution for romidepsin in patients carrying the variant alleles compared with those carrying the wild-type alleles. A similar finding has been reported with digoxin, a well-known ABCB1 substrate, where carriers of 3435T alleles had a lower peripheral volume of distribution than carriers of C alleles (32). Although the effect of the variants of *ABCB1* on various substrate drugs remain controversial, several reports in the literature suggest that one or more of the variants 1236T, 2677T/A, 3435T compose a common haplotype for *ABCB1* that confers impaired transporter expression and function (24, 26, 27). In addition to each single variant alone, we also looked at *ABCB1* diplotypes in relation to romidepsin pharmacokinetic parameters. Diplotypes were grouped to reflect an increasing order of genetic variations in the population based on an approach by Kimchi-Sarfaty and colleagues (24) as it was assumed that each additional variant allele would alter protein function and expression to a greater degree. Consideration of all the SNPs did not enhance the relationship against CL or Q that were seen with 2677G>T/A transition alone. For the peripheral volume of distribution, however, patients carrying diplotype 5 (carrying only variant alleles at all three SNPs) were marginally likely to have a lesser extent of tissue distribution for romidepsin.

In summary, this study presents a population pharmacokinetic model of romidepsin in patients with cutaneous or relapsed peripheral T-cell lymphoma who received a 4-hours infusion at the dose of 14 or 18 mg/m^2 during their first treatment cycle. The disposition of romidepsin was well-characterized by the two-compartment model with a linear elimination and exhibited moderate interpatient variabilities. No statistically significant association was found between romidepsin pharmacokinetics and patient-specific covariates including polymorphic variations in *CYP3A4/5*, *ABCB1*, or *SLCO1B3* in this population.

Disclosure of Potential Conflicts of Interest

No potential conflicts of interest were disclosed.

References

1. Ueda H, Nakajima H, Hori Y, et al. FR901228, a novel antitumor bicyclic depsipeptide produced by Chromobacterium violaceum No. 968. I. Taxonomy, fermentation, isolation, physico-chemical and biological properties, and antitumor activity. J Antibiot (Tokyo) 1994;47:301–10.
2. Ueda H, Manda T, Matsumoto S, et al. FR901228, a novel antitumor bicyclic depsipeptide produced by Chromobacterium violaceum No. 968. III. Antitumor activities on experimental tumors in mice. J Antibiot (Tokyo) 1994;47:315–23.
3. Fronsdal K, Saatcioglu F. Histone deacetylase inhibitors differentially mediate apoptosis in prostate cancer cells. Prostate 2005;62:299–306.
4. Ito T, Ouchida M, Morimoto Y, et al. Significant growth suppression of synovial sarcomas by the histone deacetylase inhibitor FK228 *in vitro* and *in vivo*. Cancer Lett 2005;224:311–9.
5. Marks P, Rifkind RA, Richon VM, Breslow R, Miller T, Kelly WK. Histone deacetylases and cancer: causes and therapies. Nat Rev Cancer 2001;1:194–202.
6. Piekarz RL, Frye AR, Wright JJ, et al. Cardiac studies in patients treated with depsipeptide, FK228, in a phase II trial for T-cell lymphoma. Clin Cancer Res 2006;12:3762–73.
7. Stadler WM, Margolin K, Ferber S, McCulloch W, Thompson JA. A phase II study of depsipeptide in refractory metastatic renal cell cancer. Clin Genitourin Cancer 2006;5:57–60.
8. Fouladi M, Furman WL, Chin T, et al. Phase I study of depsipeptide in pediatric patients with refractory solid tumors: a children's oncology group report. J Clin Oncol 2006;24:3678–85.
9. Sandor V, Bakke S, Robey RW, et al. Phase I trial of the histone deacetylase inhibitor, depsipeptide (FR901228, NSC 630176), in patients with refractory neoplasms. Clin Cancer Res 2002;8:718–28.
10. Byrd JC, Marcucci G, Parthun MR, et al. A phase 1 and pharmacodynamic study of depsipeptide (FK228) in chronic lymphocytic leukemia and acute myeloid leukemia. Blood 2005;105:959–67.
11. Piekarz RL, Robey R, Sandor V, et al. Inhibitor of histone deacetylation, depsipeptide (FR901228), in the treatment of peripheral and cutaneous T-cell lymphoma: a case report. Blood 2001;98:2865–8.
12. Marshall JL, Rizvi N, Kauh J, et al. A phase I trial of Depsipeptide (FR901228) in patients with advanced cancer. J Exp Ther Oncol 2002;2:325–32.
13. Shiraga T, Tozuka Z, Ishimura R, Kawamura A, Kagayama A. Identification of cytochrome P450 enzymes involved in the metabolism of FK228, a potent histone deacetylase inhibitor, in human liver microsomes. Biol Pharm Bull 2005;28:124–9.
14. Lee JS, Paull K, Alvarez M, et al. Rhodamine efflux patterns predict P-glycoprotein substrates in the National Cancer Institute drug screen. Mol Pharmacol 1994;46:627–38.
15. Treiber A, Schneiter R, Hausler S, Stieger B. bosentan is a substrate of human OATP1B1 and OATP1B3: inhibition of hepatic uptake as the common mechanism of its interactions with cyclosporin A, rifampicin, and sildenafil. Drug Metab Dispos 2007;35:1400–7.
16. Fehrenbach T, Cui Y, Faulstich H, Keppler D. Characterization of the transport of the bicyclic peptide phalloidin by human hepatic transport proteins. Naunyn Schmiedebergs Archives Pharmacol 2003;368:415–20.
17. Chen X, Gardner ER, Figg WD. Determination of the cyclic depsipeptide FK228 in human and mouse plasma by liquid chromatography with mass-spectrometric detection. J Chromatogr B 2008;865:153–8.
18. Sissung TM, Baum CE, Deeken J, et al. ABCB1 genetic variation influences the toxicity and clinical outcome of patients with androgen independent prostate cancer treated with docetaxel. Clin Cancer Res. 2008;14:4543–9.
19. Lepper ER, Baker SD, Permenter M, et al. Effect of common CYP3A4 and CYP3A5 variants on the pharmacokinetics of the cytochrome P450 3A phenotyping probe midazolam in cancer patients. Clin Cancer Res 2005;11:7398–404.
20. Hamada A, Sissung TM, Price DK, et al. Effect of SLCO1B3 haplotype on testosterone transport and clinical outcome in Caucasian patients with androgen-independent prostatic cancer. Clin Cancer Res 2008;14:332–80.
21. Beal SL, Sheiner LB, Boeckmann AJ. NONMEM users guides. Ellicott City, MD: Icon Development Solutions; 1989–2006.
22. Byon W, Fletcher CV, Brundage RC. Impact of censoring data below an arbitrary quantification limit on structural model misspecification. J Pharmacokinet Pharmacodyn 2008;35:101–16.
23. Yano Y, Beal SL, Sheiner LB. Evaluating pharmacokinetic/pharmacodynamic models using the posterior predictive check. J Pharmacokinet Pharmacodyn 2001;28:171–92.
24. Kimchi-Sarfaty C, Oh JM, Kim IW, et al. A "silent"

polymorphism in the MDR1 gene changes substrate specificity. Science New York (NY) 2007; 315:525–8.

25. Sissung TM, Mross K, Steinberg SM, et al. Association of ABCB1 genotypes with paclitaxel-mediated peripheral neuropathy and neutropenia. Eur J Cancer 2006;42:2893–6.

26. Kato M, Fukuda T, Serretti A, et al. ABCB1 (MDR1) gene polymorphisms are associated with the clinical response to paroxetine in patients with major depressive disorder. Prog Neuro Psychopharmacol Biol Psych 2008;32:398–404.

27. Kim RB, Leake BF, Choo EF, et al. Identification of functionally variant MDR1 alleles among European Americans and African Americans. Clin Pharmacol Ther 2001;70:189–99.

28. Baker S, Verweij J, Cusatis G, et al. Pharmacogenetic Pathway Analysis of Docetaxel Elimination. Clin Pharmacol Ther 2008;85:155–63.

29. Song P, Lamba JK, Zhang L, et al. G2677T and C3435T genotype and haplotype are associated with hepatic ABCB1 (MDR1) expression. J Clin Pharmacol 2006;46:373–9.

30. Hoffmeyer S, Burk O, von Richter O, et al. Functional polymorphisms of the human multidrug-resistance gene: multiple sequence variations and correlation of one allele with P-glycoprotein expression and activity *in vivo*. Proc Natl Acad Sci U S A 2000;97:3473–8.

31. Meissner K, Jedlitschky G, Meyer zu Schwabedissen H, et al. Modulation of multidrug resistance P-glycoprotein 1 (ABCB1) expression in human heart by hereditary polymorphisms. Pharmacogenet 2004; 14:381–5.

32. Comets E, Verstuyft C, Lavielle M, Jaillon P, Becquemont L, Mentre F. Modelling the influence of MDR1 polymorphism on digoxin pharmacokinetic parameters. Eur J Clin Pharmacol 2007;63: 437–49.

Clinical Cancer Research

Population Pharmacokinetics of Romidepsin in Patients with Cutaneous T-Cell Lymphoma and Relapsed Peripheral T-Cell Lymphoma

Sukyung Woo, Erin R. Gardner, Xiaohong Chen, et al.

Clin Cancer Res 2009;15:1496-1503.